Journal of Sound and Vibration (1996) **198**(1), 81–94

A MODIFIED H_2 FEEDFORWARD ACTIVE CONTROL SYSTEM FOR SUPPRESSING BROADBAND RANDOM AND TRANSIENT NOISES

M. Bai and H. Chen

Department of Mechanical Engineering, Chiao-Tung University, 1001 *Ta-Hsueh Road*, *Hsin-Chu* 30050 *Taiwan*, *Republic of China*

(*Received* 2 *November* 1995, *and in final form* 16 *April* 1996)

Three feedforward active noise control algorithms based on H_2, H_∞, and modified H_2 optimal model matching principles are investigated in this study. The first two methods provide significant attenuation for broadband random noises. However, the H_2 and H_∞ methods generally result in high-gain controllers at high frequencies, which calls for some truncation measures in the frequency domain. The third method effectively eliminates the high-gain problem of the ordinary H_2 and H_∞ algorithms. In addition, this method is guaranteed to result in a causal and stable controller which is crucial in practical implementation. The algorithms are coded into controllers by using a floating-point digital signal processor. The experimental results show significant attenuation for stationary broadband random noises as well as transient impact noises in a duct.

1. INTRODUCTION

Active noise control (ANC) techniques serve as a useful alternative to conventional passive control methods because it provides numerous advantages such as improved low-frequency performance, reduction of size and weight, zero back pressure, reduction of energy consumption, and programmable flexibility of design [1]. A vast amount of literature has been produced in the last decade and a very good review can be found in Reference [2]. In the ANC configurations up to date, feedforward control has become the most widely used one (whenever the upstream reference signal is available) because it generally provides better performance in suppressing broadband noises within a moderate controller gain than the feedback control [2].

In this study, three feedforward active noise control algorithms based on H_2, H_∞, and modified H_2 optimal model matching principles are investigated. These methods effectively overcome the problem of the unstable inverse plant resulting from the inherent non-minimum phase (NMP) property of the cancellation path. The NMP behavior is a fundamental issue which is at the heart of the control system design, but often an overlooked factor that could seriously degrade the ANC performance in attenuating broadband random noises. Despite the effectiveness, the H_2 and H_∞ methods generally result in high-gain controllers at high frequencies, which calls for some truncation measures in the frequency domain during the controller design stage. To ease the problem, a modified H_2 method has been developed to reduce the controller gain of the ordinary H_2 and H_∞ algorithms. In addition, this method is guaranteed to result in a causal and stable controller which is crucial in practical implementation. The feedforward algorithms are coded into ANC controllers by using a floating-point digital signal processor (DSP).

0022–460X/96/460081 + 14 $25.00/0

The experimental results show significant attenuation for stationary broadband random noises in a duct. The proposed methods also have potential in suppressing transient impact noises that have been the major difficulty to adaptive methods.

Experiments are performed on a duct of finite length to justify the proposed methods. The experimental results obtained by using the H_2 and H_∞ feedforward techniques show comparable attenuation for stationary noises as the popular filtered-x least mean square (LMS) method [3, 4]. The proposed methods also have potential in suppressing transient noises, e.g., the impact of a forge hammer.

This paper is organized as follows. First, the ANC algorithms based on H_2 and H_∞ optimization criteria will be briefly described. Then, a modified H_2 method will be developed for alleviating the high-gain problem associated with the ordinary H_2 and H_∞ methods. In the following sections, the techniques developed will be validated by experimental investigations and the methods compared. In the final section, a conclusion of this work will be given.

2. THE ORDINARY H_2 AND H_∞ FEEDFORWARD ANC ALGORITHMS

In the sequel, the formulations are expressed in terms of sampled-data systems and discrete-time base to facilitate the presentation and the digital implementation of the ANC algorithms. Consider the feedforward ANC problem of a finite-length duct, as shown in Figure 1. The sampled signal $x(k)$ is the input disturbance noise. $P(z)$ is the transfer function of the primary acoustic plant, where z denotes the z-transform variable. $S(z)$ is the transfer function of the cancellation path composed of the actuator, the acoustic error path, and the sensor. This problem can be posed into a model matching problem, where the ANC problem amounts to finding the controller $C(z)$ such that the residual field $y(k)$ can be minimized. In order to match the characteristics of the paths $P(z)$, $C(z)$ and $S(z)$, one is tempted to set

$$C(z) = -P(z)/S(z). \tag{1}$$

However, it frequently occurs that $S(z)$ is NMP, where direct application of equation (1) leads to a non-causal or unstable controller which is not implementable. It is then highly desirable to develop an ANC method that would effectively match the primary path and the cancellation path with respect to some optimal criteria when the NMP behavior is an issue. In this paper, two model matching algorithms capable of dealing with NMP problems in ANC applications are described.

The first approach is based on the H_2 optimal criterion. Since the feedforward ANC problem is equivalent to matching the characteristics of the primary path and the cancellation path, the degree of match can be measured using various criteria. The criterion

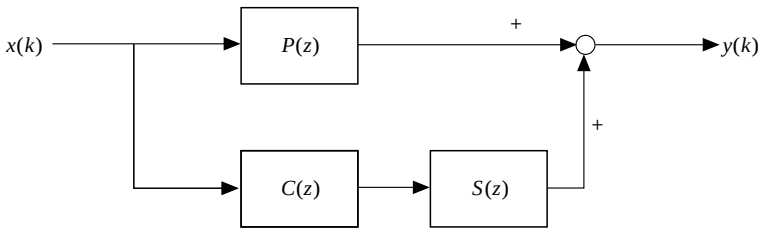

Figure 1. System block diagram of the feedforward ANC problem. $P(z)$, $S(z)$, and $C(z)$ are the discrete-time transfer functions of the primary acoustic path, the secondary path, and the controller, respectively.

employed in the following method is the 2-norm in the Hilbert space. The squared error ε_2^2 is defined as follows:

$$\varepsilon_2^2 = \| P(z) + C(z)S(z) \|_2^2, \tag{2}$$

where the 2-norm of a scalar transfer function is defined as

$$\| G(z) \|_2 \triangleq \left(\frac{1}{2\pi} \int_{-\pi}^{\pi} |G(e^{j\theta})|^2 \, d\theta \right)^{1/2} \tag{3}$$

The feedforward model matching problem then reduces to finding a biproper and stable transfer function (z) to minimize ε_2^2. The following derivation entails the so-called *inner-outer* factorization. It can be shown that every proper and stable function $T(z)$ has a factorization [5]

$$T(z) = T_a(z)T_m(z) \tag{4}$$

with $T_a(z)$ being an all-pass function and $T_m(z)$ being a biproper minimum phase function. By assuming that the transfer function $S(z)$ has been factored accordingly as $S(z) = V_a(z)V_m(z)$ and substituting the factored form into equation (2) and omiting (z) for simplicity one obtains

$$\varepsilon_2^2 = \| P + V_a V_m C \|_2^2 = \| V_a V_a^{-1} P + V_a V_m C \|_2^2 = \| V_a (V_a^{-1} P + V_m C) \|_2^2 = \| V_a^{-1} P + V_m C \|_2^2 \tag{5}$$

In the last step, V_a has a bounded constant magnitude on the unit circle. In Hilbert space, $V_a^{-1}P$ can be uniquely decomposed into a stable part and an unstable part (by partial fraction expansion)

$$V_a^{-1} P = (V_a^{-1} P)_+ + (V_a^{-1} P)_-, \tag{6}$$

where $(V_a^{-1}P)_+$, and $(V_a^{-1}P)_-$ correspond to the unstable part and the stable part respectively. Note as these two terms belong to the subspaces that are orthogonal complements to each other. Then equation (5) can be developed into

$$\varepsilon_2^2 = \| (V_a^{-1} P)_+ + (V_a^{-1} P)_- + V_m C \|_2^2 = \| (V_a^{-1} P)_+ \|_2^2 + \| (V_a^{-1} P)_- + V_m C \|_2^2 \tag{7}$$

The Pythagoras theorem in Hilbert space was used in the last equality. It is now clear that the unique optimal C_{opt} (z) is

$$C_{opt}(z) = - V_m^{-1} (V_a^{-1} P)_s \tag{8}$$

and the minimum of ε_2^2 equals $\| (V_a^{-1}P)_u \|_2^2$. Note that this minimum value dictates the ultimately achievable performance imposed by the NMP constraint.

Another elegant approach to match the characteristics of the primary path and the cancellation path is based on the H_∞ optimal criterion. The ∞-norm of a scalar transfer function $G(z)$ is defined as

$$\| G(z) \|_\infty = \sup_{\theta \in (-\pi, \pi)} |G(e^{j\theta})|, \tag{9}$$

where sup denotes the least upper bound. As with the H_2-norm optimization, the feedforward ANC problem can be recast into that of finding a biproper and stable transfer function $C(z)$ to minimize the ∞-norm error

$$\varepsilon_\infty = \| P + SC \|_\infty. \tag{10}$$

The problem can now be formulated in terms of the ∞-norm as

$$\begin{aligned}\min \| P + SC \|_\infty &= \min \| P + V_a V_m C \|_\infty = \min \| V_a V_a^{-1} P + V_a V_m C \|_\infty \\ &= \min \| V_a (V_a^{-1} P + V_m C) \|_\infty = \min \| V_a^{-1} P + V_m C \|_\infty \end{aligned} \tag{11}$$

where the inner-outer expansion of the transfer function $S(z)$ and the property of the all-pass function $|V_a(e^{j\theta})| = 1$, $\theta \in (-\pi, \pi]$ have been used.

Next, define $R = V_a^{-1} P$ and $Q = -V_m C$. The problem in equation (13) is then reduced to finding a stable and proper $Q(z)$ for a given proper (not necessarily stable) $R(z)$ such that $\| R - Q \|_\infty$ is minimized. This is the well-known Nahari problem and the minimum value can be shown to be the Hankel norm of the operator R [6].

A state space method is employed in this paper for solving the Nahari problem [6]. To keep the presentation to a reasonable length, the procedure of finding the optimal transfer functions $Q(z)$ and $C(z)$ is summarized as follows. In this algorithm *packed* matrix notation is used to denote the state-space realization, i.e., $\mathbf{x}(k+1) = \mathbf{A}\mathbf{x}(k) + \mathbf{B}u(k)$, $y(k) = \mathbf{C}\mathbf{x}(k) + Du(k)$ is denoted as $[\mathbf{A}, \mathbf{B}, \mathbf{C}, D]$.

(1) Find the inner-outer factorization of the cancellation path: $S(z) = V_a(z) V_m(z)$ with both $V_m(z)$ and $V_m^{-1}(z)$ being proper and stable. (2) Find a minimal realization of $R(z)$ and separate it into the stable part and the unstable part $R(z) = [\mathbf{A}, \mathbf{B}, \mathbf{C}, 0] +$ (stable part). (3) Solve the discrete-time Lyapunov equations for the controllability grammian $\mathbf{L}_c$ and the observability grammian $\mathbf{L}_o$. $\mathbf{L}_c - \mathbf{A}\mathbf{L}_c\mathbf{A}^{\mathrm{T}} = \mathbf{B}\mathbf{B}^{\mathrm{T}}$; $\mathbf{L}_o - \mathbf{A}^{\mathrm{T}}\mathbf{L}_o\mathbf{A} = \mathbf{C}^{\mathrm{T}}\mathbf{C}$. (4) Find the maximum eigenvalue λ^2 of $\mathbf{L}_c\mathbf{L}_o$ and a corresponding eigenvector $\mathbf{w}$. (5) Define $f(z) = [\mathbf{A}, \mathbf{w}, \mathbf{C}, 0]$; $g(z) = [-\mathbf{A}^{\mathrm{T}}, \lambda^{-1}, \mathbf{L}_o\mathbf{w}, \mathbf{B}^{\mathrm{T}}, 0]$. (6) Set $Q_{opt}(z) = R(z) - \lambda f(z)/g(z)$. (7) Calculate the optimal controller $C_{opt}(z) = -V_m^{-1}(z) Q_{opt}(z)$.

It should be noted that, unlike the H_2 method, the H_∞ method *per se* is to achieve model matching in an optimal way subject to the *worst-case* input [5]. The optimization of the H_∞ method is carried out for the whole class of input with bounded energy. Thus, the H_∞ method tends to be more conservative than the H_2 method in terms of performance.

3. THE MODIFIED H_2 FEEDFORWARD ANC ALGORITHM

As presented earlier, the H_2 and H_∞ methods effectively solve the model matching problem, even if the NMP problem of the plant is present. However, this masks somewhat a pitfall of the above methods. More precisely, excessive compensation for the NMP zeros by using the H_2 and H_∞ methods will generally result in unnecessary high gains at high frequencies. The fact that the NMP zeros cluster at high frequencies is common for physical systems with flexibility [7], but other than that, it is more often than not the consequence of discretization of analog plants [8]. Compensation for these artificially generated NMP zeros is sometimes not worth the effort because the uncertainty of the NMP zeros obtained by experimental system identification methods is generally large at the plant zeros, where the plant output is extremely small. The NMP zeros impose inherent design constraints on the controller, wherein high-gains at high frequencies become inevitable. In practical implementation of the ANC controller, the effect of high-gains at high frequencies is very detrimental since they will saturate the actuator and one should avoid them whenever possible.

To alleviate the problem caused by the NMP zeros at high frequencies, remedies must be sought for designing the controller by using the H_2 and H_∞ principles. Unfortunately, a standard procedure of rolling-off by a low-pass filter stated in robust control literature [5, 9] would not seem to work for the present extremely high-order acoustic system (usually above 50). This is because the low-pass filter not only attenuates the high-frequency

magnitude but also introduces considerable phase shift that destroys the optimality of the controller. In practice, it is very difficult if not impossible to find a satisfactory compromise between the roll-off of magnitude and the invariance of phase, as manifested by Bode's magnitude-phase relationship [10]. Hence, an alternative is employed in the present study to sample the frequency response function of the resulting controller and truncate the high-frequency portion. Then, the truncated frequency response function is inverse discrete Fourier transformed to yield the impulse response function which amounts to the coefficients of the finite impulse response (FIR) filter of the ANC controller. The reduced-gain controller can thus be safely used without saturating the actuator. Although the method should work for any stable system as it does in the present case, this heuristic approach is not based on any sort of optimality. In the sequel, a modified H_2 algorithm will be developed to eliminate the high-gain problem in a more elegant way.

In the proposed method, a key to elimating the high-gain problem is to introduce a constraint on the controller gain. This is done by modifying the 2-norm cost function in equation (2) into the following form:

$$J = \| [P(z) + C(z)S(z)] \|_2^2 + r \| C(z) \|_2^2, \tag{12}$$

where r is a weighting parameter which stipulates the relative importance of the control error and control effort. A large value of r corresponds to *expensive* control, while a small value corresponds to *cheap* control. Minimization of the cost function in equation (12) amounts to regulating the system response as close to the zero error of model matching while, on the other hand, keeping the gain of the controller as low as possible.

Using Parseval's theorem in the z-domain, the cost function in equation (12) can be rewritten as

$$J = \frac{1}{2\pi j} \oint_{|z|=1} \{[P(z) + C(z)S(z)][p(z^{-1}) + C(z^{-1})S(z^{-1})] + rC(z)C(z^{-1})\} z^{-1} \, \mathrm{d}z \tag{13}$$

The stationary point of the cost function can be found by taking the first variation of J.

$$\delta J = \frac{1}{2\pi j} \oint_{|z|=1} \{S(z)[P(z^{-1}) + C(z^{-1})S(z^{-1})] \, \delta C(z) + S(z^{-1})[P(z) + C(z)S(z)] \, \delta C(z^{-1})$$

$$+ rC(z) \, \delta C(z^{-1}) + rC(z) \, \delta C(z^{-1})\} z^{-1} \, \mathrm{d}z = 0 \tag{14}$$

Noting that, in the integrand, the terms associated with $\delta C(z)$ and $\delta C(z^{-1})$ are symmetrical enables equation (14) to be simplified into

$$\delta J = \frac{1}{\pi j} \oint_{|z|=1} [P(z)S(z^{-1}) + C(z)S(z)S(z^{-1}) + rC(z)] \, \delta C(z^{-1}) z^{-1} \, \mathrm{d}z = 0 \tag{15}$$

Before explicitly finding the solution of the optimal $C(z)$, one first checks if the stationary point is a minimum by taking the second variation of J.

$$\delta^2 J = \frac{1}{\pi j} \oint_{|z|=1} [S(z)S(z^{-1}) + r][\delta C(z^{-1})]_2 z^{-1} \, \mathrm{d}z \tag{16}$$

Let the plant $S(z)$ be a proper and stable real rational function:

$$S(z) = N(z)/D(z). \tag{17}$$

Then

$$S(z)S(z^{-1}) + r = D^*(z)D^*(z^{-1})/D(z)D(z^{-1}), \tag{18}$$

where $D^*(z)$ is obtained from the following spectral factorization:

$$D^*(z)D^*(z^{-1}) = N(z)N(z^{-1}) + rD(z)D(z^{-1}) \tag{19}$$

with $D^*(z)$ and $D^*(z^{-1})$ containing all roots inside and outside respectively, the unit circle $|z| = 1$. It is easy to verify that, if $r \neq 0$, $D^*(z)D^*(z^{-1})$ has no root on the unit circle, and all roots are reciprocal. Thus, by substituting equation (18) into equation (16), the second variation of the cost function can be expressed

$$\delta^2 J = \frac{1}{\pi} \int_0^{2\pi} \frac{|D^*(\mathrm{e}^{j\theta})|^2}{|D(\mathrm{e}^{j\theta})|^2} [\delta C(\mathrm{e}^{j\theta})]^2 \, \mathrm{d}\theta \tag{20}$$

which is strictly positive and this confirms that the stationary point of the cost function is indeed the minimum.

Now one is in a position to solve equation (15) for the optimal controller. This can be accomplished by requiring the poles of the integrand to be strictly outside the unit circle. Let the integrand $X(z)$ in equation (15) be expressed as

$$X(z) = C(z)F(z)F(z^{-1})z^{-1} + P(z)S(z^{-1})z^{-1}, \tag{21}$$

where

$$F(z) = D^*(z)/D(z) \tag{22}$$

whose poles are strictly inside the unit circle. For convenience, denote this by $F(z) \subset \mathbf{C}_-$, where $\mathbf{C}_-$ stands for the set of all real rational transfer functions with poles strictly inside the unit circle. Set $\mathbf{C}_+$ may also be needed to indicate the complementary set of all real rational transfer functions with poles on or strictly outside the unit circle. With some straighforward manipulations, equation (21) leads to

$$X(z)/F(z^{-1}) - Q_+(z) = C(z)F(z)z^{-1} + Q_-(z), \tag{23}$$

where $Q_-(z) \in \mathbf{C}_-$ and $Q_+(z) \in \mathbf{C}_+$ are the stable and unstable part of $P(z)S(z^{-1})z^{-1}/F(z^{-1})$ respectively. In equation (23), since all poles on the left hand side are outside the unit circle whilst all poles on the right hand side are inside the unit circle, the two sides are therefore independent and must both be equal to zero. From the right hand side of equation (23), one obtains the optimal solution of the controller $C_{opt}(z)$:

$$\begin{aligned} C_{opt}(z) &= -zQ_-(z)/F(z) = (-zD(z)/D^*(z))[P(z)N(z^{-1})D(z^{-1})/zD(z^{-1})D^*(z^{-1})_-] \\ &= (-zD(z)/D^*(z))[P(z)N(z^{-1})/zD^*(z^{-1})_-] \end{aligned} \tag{24}$$

where $[\cdot]_- \subset \mathbf{C}_-$ denotes the stable part of a transfer function. If $r \neq 0$, it is easy to verify that the optimal controller in equation (24) is guaranteed to be causal and stable, which is crucial in on-line and real-time ANC implementations. It is also straighforward to show that the optimal controller will reduce to the ordinary H_2 controller if $r = 0$ and to the simple controller in equation (1) if, in addition, $S(z)$ is the minimum phase. In summary, given the characteristics of the primary path and the secondary path, one may choose an

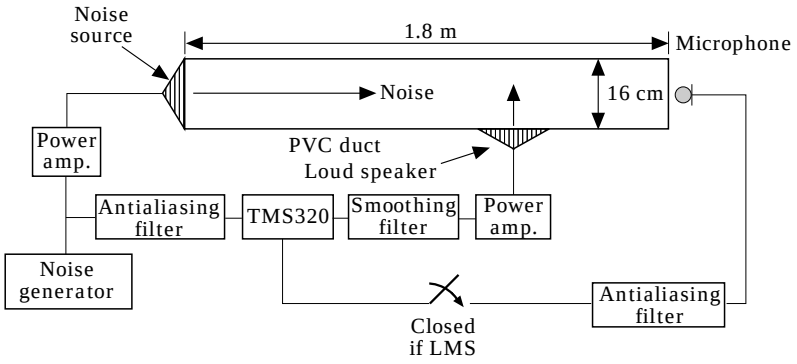

Figure 2. Experimental setup of the ANC system for a duct.

appropriate parameter r to calculate the modified H_2 ANC feedforward controller according to equation (24), provided that the spectral factorization in equation (19) has been obtained.

4. EXPERIMENTAL INVESTIGATIONS

Experiments were conducted to justify the developed modified H_2 feedforward ANC technique. Voltage signals are used as the reference inputs so that acoustic feedback can be ignored. The algorithms are implemented on a 32-bit floating-point digital signal processor TMS320C31 in conjunction with two-channel analog inputs and outputs. A circular PVC duct of length 1·8 m and diameter 16 cm was chosen for the test. The corresponding cutoff frequency of the duct is 1075 Hz. This renders the effective control bandwidth below approximately 1 kHz, where only plane waves are of interest. Two third order Bessel filters are used as the anti-aliasing filter and the smoothing filter, respectively. The ANC system, including the digital controller, the signal conditioning circuit, the sensor, and the actuator, is schematically shown in Figure 2. Four ANC algorithms are employed to suppress various synthetic noises and practical noises. The primary noises used in the experiments include the Guassian white noise, an engine noise, a blower noise, and an impact noise.

When implementing the digital controllers, the models of $P(z)$ and $S(z)$ must be determined prior to finding $C(z)$. To this end, a parametric system identification procedure is utilized to establish a mathematical model of the transducer-duct system. First, the sampled input signal $u(k)$ and the output signal $y(k)$ are recorded by a data acquisition system. Then a parametric model is estimated on the basis of these input and output data. The white noise is selected as the input signal since it satisfies the condition of *persistent excitation*, as required by a reliable system identification [12]. The parametric model adopted in this study is the autoregressive with exogenous input (ARX) model

$$y(k) = G(z)u(k) + H(z(e)k), \quad k = 1, 2, \ldots, \infty, \tag{25}$$

where z is the shift operator, $G(z)$ is the plant transfer function to be identified, and $H(z)$ is the transfer function associated with the disturbance process. In ARX model, the transfer functions $G(z)$ and $H(z)$ take the following forms:

$$G(z) = z^{-N}B(z^{-1})/A(z^{-1}), \qquad H(z) = 1/A(z^{-1}) \tag{26}$$

where N is the delay in samples, $A(z^{-1})$ and $B(z^{-1})$ are polynomials in z^{-1}, i.e.,

$$A(z^{-1}) = 1 + a_1 z^{-1} + \cdots + a_{na} z^{-na}, \qquad B(z^{-1}) = b_1 + b_2 z^{-1} + \cdots + b_{nb} z^{-nb+1} \tag{27}$$

with the numbers na and $nb - 1$ being the orders of the respective polynomials. Hence, the model in equation (25) can be written as

$$A(z^{-1})y(k) = B(z^{-1})u(k - nk) + e(k). \tag{28}$$

The system identification is essentially a time-domain curve-fitting procedure that estimates these $(na + nb)$ parameters in the ARX model by, for example, the least square method. Details can be found in Reference [12].

For the transducer-duct systems, the aforementioned parametric identification procedure was employed to set up the corresponding mathematical models. First, the input data (white noise) and the output data were recorded by a signal analyzer, based on a sampling rate of 4 kHz. Second, the output data were shifted and interpolated to accommodate the additional delay due to the I/O operations of the DSP. Third, the

TABLE 1

The mathematical models of the primary path and the cancellation path identified by the ARX procedure

$P(z)$		$S(z)$	
delay = 22, gain = 0·0613		delay = 16, gain = 0·2724	
zeros	poles	zeros	poles
*−7·7165	0·8685 ± 0·4815i	*−1·1551	−0·9432 ± 0·0972i
*1·0125 ± 0·0097i	0·8961 ± 0·4144i	*−1·0484 ± 0·0776i	−0·9457 ± 0·2103i
0·9244 ± 0·3464i	0·9235 ± 0·3163i	−0·9500 ± 0·2785i	−0·8412 ± 0·2888i
0·7964 ± 0·4002i	0·9505 ± 0·1799i	*−0·8852 ± 0·4751i	−0·8293 ± 0·4289i
0·5881 ± 0·7941i	0·9707 ± 0·0639i	−0·7036 ± 0·5822i	−0·8165 ± 0·4748i
0·6342 ± 0·5526i	0·7923 ± 0·5989i	*−0·6500 ± 0·7641i	−0·7489 ± 0·6045i
0·4678 ± 0·7088i	0·7155 ± 0·6874i	−0·5027 ± 0·8538i	−0·6722 ± 0·7225i
0·2576 ± 0·8202i	0·6221 ± 0·7764i	−0·2577 ± 0·9553i	−0·5889 ± 0·7888i
0·0295 ± 0·9770i	0·5365 ± 0·8248i	−0·3470 ± 0·7281i	−0·4687 ± 0·8662i
−0·1063 ± 0·8638i	0·4744 ± 0·8684i	−0·0831 ± 0·9795i	−0·3308 ± 0·9195i
−0·2989 ± 0·8328i	0·3361 ± 0·9300i	0·1146 ± 0·9880i	−0·2214 ± 0·9537i
−0·5678 ± 0·7791i	0·2201 ± 0·9597i	0·2972 ± 0·9535i	−0·0851 ± 0·9640i
−0·9672	0·0888 ± 0·9885i	0·4637 ± 0·8560i	0·0044 ± 0·9789i
−0·8975 ± 0·2670i	−0·0072 ± 0·9647i	0·6366 ± 0·7678i	0·0879 ± 0·9816i
−0·8004 ± 0·4315i	−0·0737 ± 0·9836i	0·7674 ± 0·6358i	0·2164 ± 0·9564i
−0·6730 ± 0·5743i	−0·2191 ± 0·9520i	*1·0190 ± 0·0087i	0·3335 ± 0·9264i
−0·3959 ± 0·6569i	−0·3256 ± 0·9223i	0·9446 ± 0·2904i	0·4628 ± 0·8351i
−0·2394	−0·4623 ± 0·8605i	0·8720 ± 0·4686i	0·5382 ± 0·8238i
	−0·5629 ± 0·8007i	0·5244 ± 0·4154i	0·6214 ± 0·7717i
	−0·6032 ± 0·7403i		0·7165 ± 0·6872i
	−0·6757 ± 0·6740i		0·7926 ± 0·5979i
	−0·7665 ± 0·5842i		0·8637 ± 0·4759i
	−0·8254 ± 0·4690i		0·8984 ± 0·4143i
	−0·8650 ± 0·3833i		0·9323 ± 0·3004i
	−0·9041 ± 0·2615i		0·9542 ± 0·1953i
	−0·8834 ± 0·2204i		0·9838 ± 0·0588i
	−0·9570 ± 0·0480i		0·9838 ± 0·0588i
	−0·9518		−0·0493

* Denotes non-minimum phase zeros.

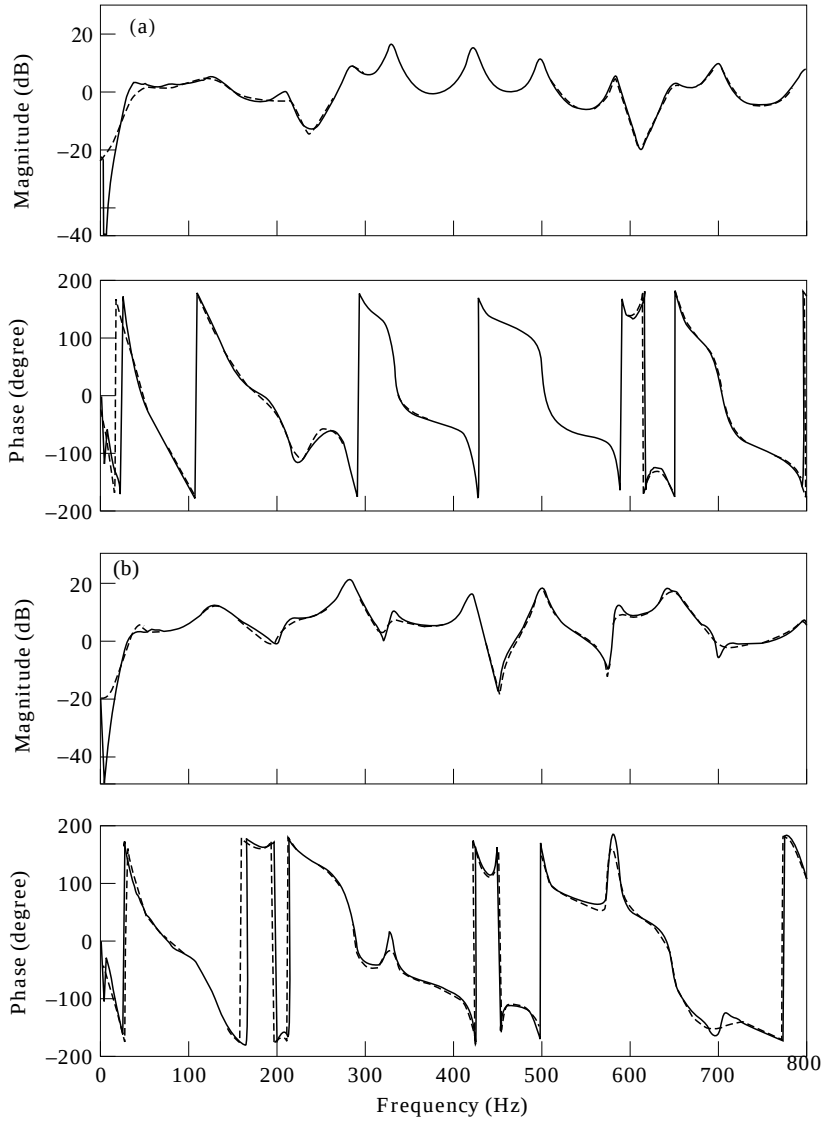

Figure 3. Comparison between the measured and the regenerated freqency response functions. (a) Frequency response function between the primary noise and the sensor: $P(e^{j\omega})$; (b) frequency response function between the canceling loudspeaker and the sensor: $S(e^{j\omega})$. ——, Measured data; ----, regenerated data.

coefficients of the ARX model were estimated by choosing appropriate orders and the delay. This process might take several iterations until the magnitude and the phase of the measured and the regenerated frequency response functions were well matched and the ARX model orders were selected according to the Akaike's information theoretical criterion (AIC) [12]. The poles and zeros of the transfer functions of the primary path and the cancellation path identified by using the ARX model are shown in Table 1 and their frequency response functions are shown in Figure 3. Note that there are 9 NMP zeros in the plant $S(z)$. Comparison of the system delays between the two paths reveals that the causality was not violated, which is critical for feedforward ANC configurations. Excellent agreement was obtained between the measured and the regenerated frequency response

functions except for the frequency range below approximately 50 Hz, where the low-frequency responses of the loudspeakers were poor. Consequently, the control bandwidth was restricted to approximately 50–800 Hz. To show the effectiveness of the modified H_2 formulation for reducing the high frequency gain, the magnitudes of the controller frequency responses obtained from the H_2 method, the H_∞ method, and the modified H_2 methods ($r = 0{\cdot}01$ and 1 respectively) are compared in Figure 4. The ordinary H_2 and H_∞ methods led to high gains above approximately 1·2 kHz, which would saturate the actuator. On the other hand, the modified H_2 method indeed resulted in an optimal controller with moderate gain at high frequencies and it could be implemented readily by using either an IIR filter or an FIR filter. Naturally, the cost of reducing the gain at high frequencies by choosing a large r value, e.g., $r = 1$ in the above case, was some degradation at the low frequencies. In the sequel, the results obtained from five ANC experiments will be presented.

In the first case, a Gaussian white noise was used as the primary noise. The H_2 method, the H_∞ method, the modified H_2 method, and the filtered-x LMS method were compared. In this case, the ordinary H_2 and H_∞ methods were implemented by 768-tapped FIR filters because of the high-gain problem. The procedure of frequency truncation has been given previously. In the filtered-x LMS method, the filter length was 256 and the step size was 0·01. The sound pressure spectra (20 averages) before and 2 min after ANC was activated are shown in Figure 5. The total noise attenuation in the band 50–800 Hz obtained by using the H_2 method, the H_∞ method, the modified H_2 method, and the filtered-x LMS method was found to be 9·3 dB, 7·3 dB, 9·5 dB, and 6·2 dB respectively. Among the methods, the H_2 method and the modified H_2 method appeared to provide the best attenuation of the broadband random noise, especially at low frequencies (approximately 10–25 dB at 50–200 Hz).

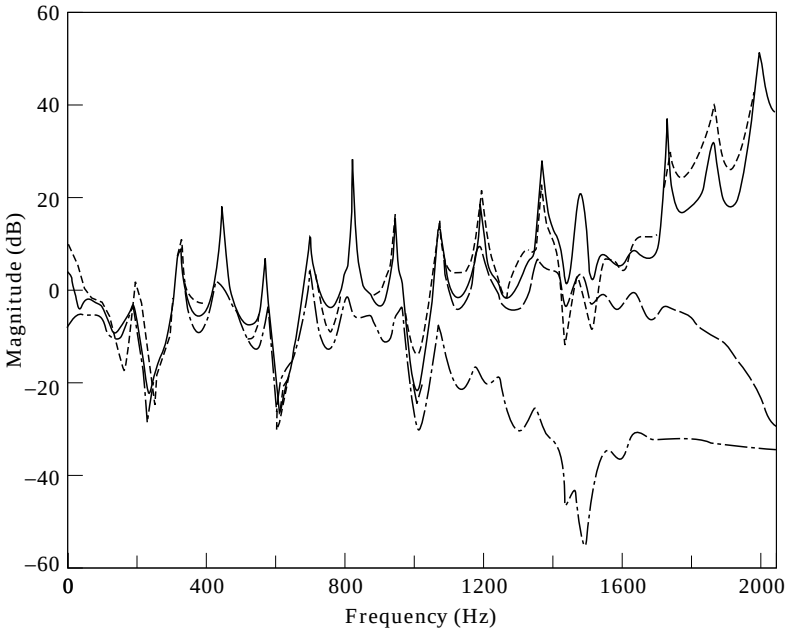

Figure 4. The magnitudes of the controller frequency responses obtained from the feedforward ANC methods. ——, H_2; – – – H_∞; — · — modified H_2 ($r = 0{\cdot}01$); — — — modified H_2 ($r = 1$).

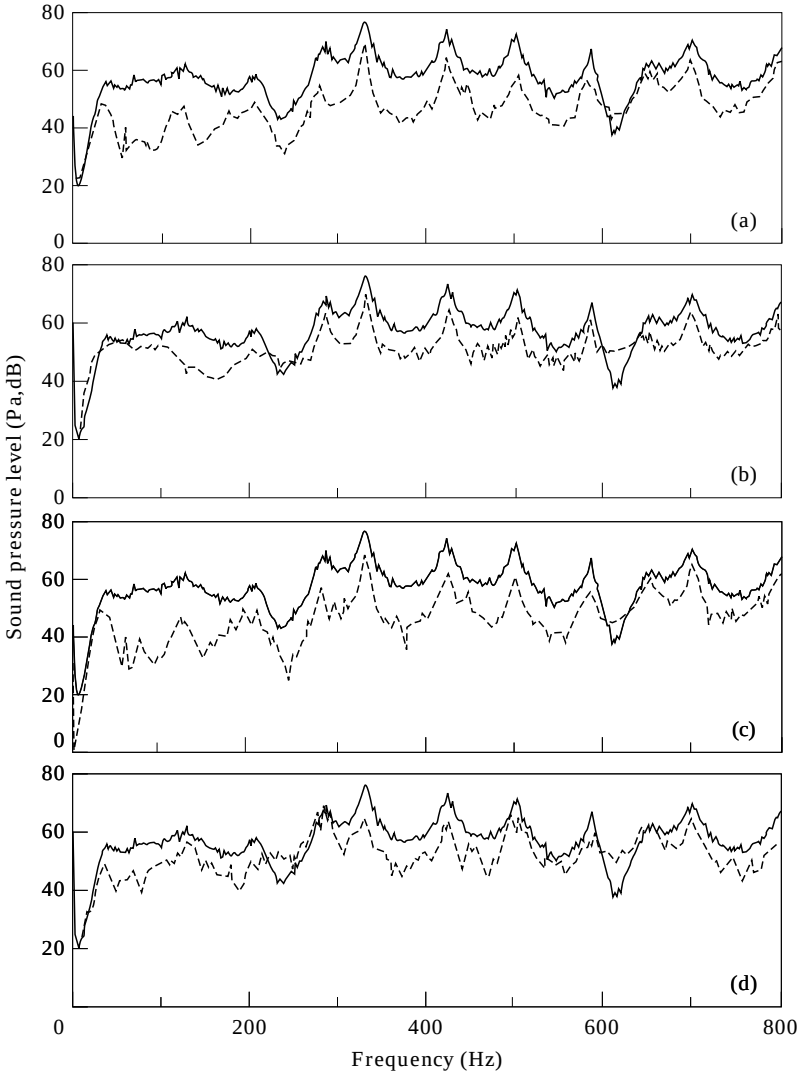

Figure 5. The sound pressure spectra for the Gaussian white noise before and after ANC was activated. (a) H_2 method; (b) H_∞ method; (c) modified H_2 method; (d) filtered-x LMS method. The step size used in filtered-x LMS was 0·01, the filter length is 256, and the result was obtained 2 min after the algorithm was activated. ——, Before control; ----, after control.

In the second case, an exhaust noise from the gasoline engine of a 2 l car operating at 4000 rpm was chosen as a more practical primary noise. To save space, only the results (20 averaged power spectra of sound pressure) obtained from the modified H_2 method and the filtered-x LMS method are shown in Figure 6. The total noise attenuation obtained from the modified H_2 method and filtered-x LMS method appeared to give more attenuation at larger peaks (due to the problem of eigenvalue disparity [13]), while the modified H_2 method yielded attenuation throughout the band.

In the third case, the noise from a blower with a radial fan operating at 3000 r.p.m was used as the primary noise. The noise contained harmonics associated with the blade-passing frequency and broadband components due to turbulence. The results (20 averaged per spectra of sound pressure) obtained from the modified H_2 method and the

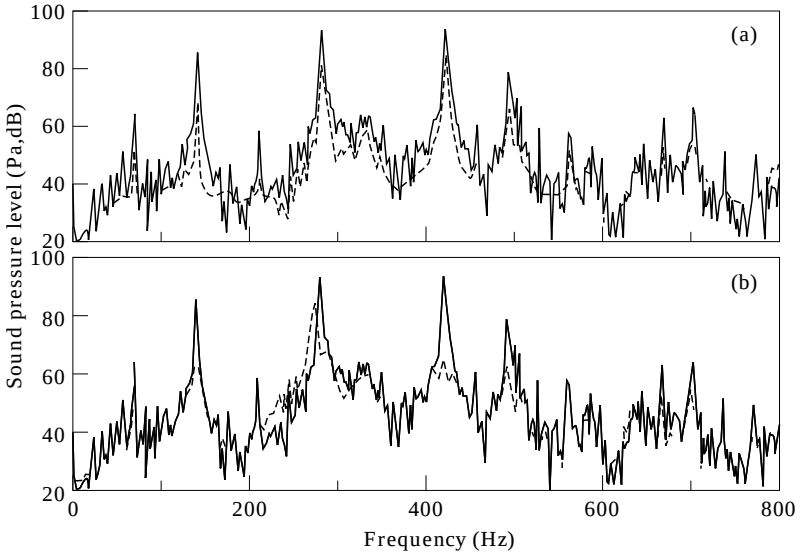

Figure 6. The sound pressure spectra for the engine noise of a car before and after ANC was activated. (a) Modified H_2 method; (b) filtered-x LMS method. The step size used in the filtered-x LMS was 0·005, the filter length was 256, and the result was obtained 2 min after the algorithms was activated. ——, Before control; ----, after control.

filtered-x LMS method is shown in Figure 7. The total noise attenuation of the modified H_2 method and the filtered-x LMS method was found to be 9·9 dB and 8·3 dB respectively.

In the final case, an impact noise from a forge hammer in a shipyard was chosen as the primary noise. The reason for choosing the impact noise is because it represents a large class of transient noises. For example, the impact noise of punch presses, the noise of forge

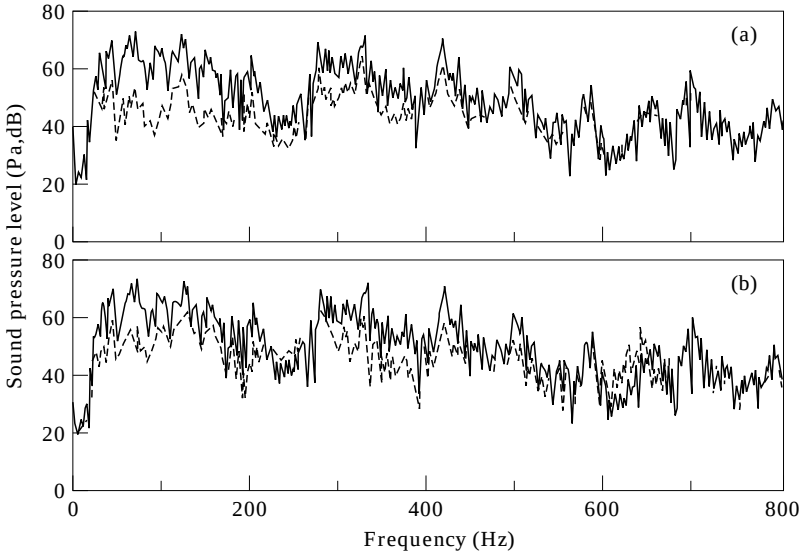

Figure 7. The sound pressure spectra for the blower noise before and after ANC was activated. (a) Modified H_2 method; (b) filtered-x LMS method. The step size in the filtered-x LMS was 0·1, the filter length was 256, and the result was obtained 2 min after the algorithm was activated. ——, Before control; ----, after control.

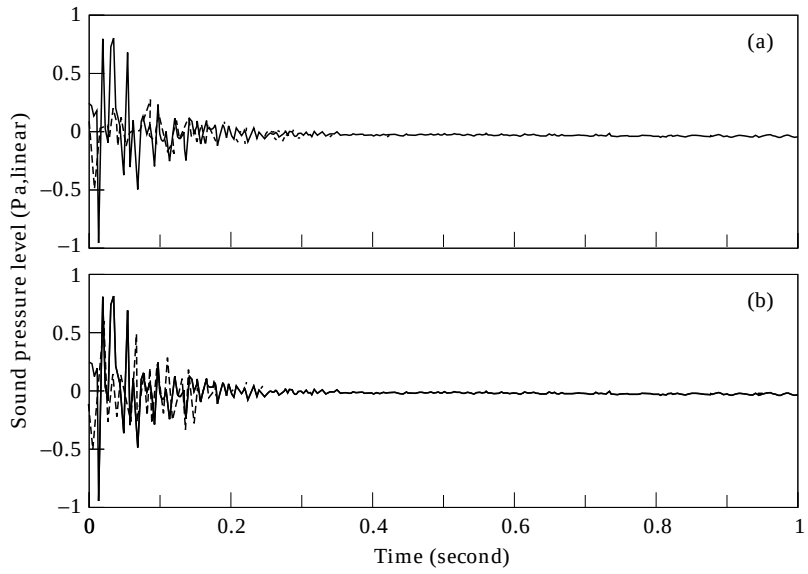

Figure 8. The time-domain response for the impact noise before and after ANC was activated. (a) Modified H_2 method; (b) filtered-x LMS method. The step size used in the filtered-x LMS was 0·05 and the filter length was 256. ——, Before control; ----, after control.

machines, the noise of gun shots, and the tunnel noise of high-speed trains all fall into this category. This particular type of application has rarely been investigated in ANC research because it involves difficulties of control methods and transduction. In the study, the authors attempted to use the modified H_2 method to attack the practical noise problem. The time-domain response of the impact noise before and after ANC was activated is shown in Figure 8. Visual comparison between the modified H_2 method and the filtered-x LMS method indicates that the former produced better performance in suppressing the impact noise than the latter. The filtered-x LMS method appeared sluggish in responding to this transient noise. The allowable adaption time in this case was too short (approximately 0·1 s) for the LMS method which requires the noise be either periodic or with slowly-varying statistics. On the other hand, the H_2 and H_∞ methods are essentially fixed controllers which do not require adaptation and therefore the control of transient noises is almost instant.

5. CONCLUSION

Three feedforward active noise control algorithms based on the H_2, the H_∞, and the modified H_2 optimal model matching principles have been developed in this study. The first two methods provide significant noise attenuation for broadband random noises at the expense of the high-gain problem. The third method effectively eliminates the high-gain problem of the ordinary H_2 and H_∞ algorithms. An ANC system for duct noises based on the feedforward algoithms has been realized by using a digital signal processor. The experimental results indicate that the proposed method provides comparable noise attenuation to the widely-used filtered-x LMS method. In addition, it exhibits great potential in actively suppressing transient noises. A limitation of the proposed method is that the performance will deteriorate if the plant drifts excessively from its normal setting, as may arise in practical applications. From this perspective, the development of adaptive

ANC algorithms based on the H_2 and H_∞ principles will be the main emphasis of future research.

ACKNOWLEDGMENTS

Special thanks are due to Professors C. Y. Chung and J. S. Hu for the helpful discussions on the H_2 and H_∞ control theories. The work was supported by the National Science Council in Taiwan, Republic of China, under project number NSC 83-0401-E009-024.

REFERENCES

1. P. A. Nelson and S. J. Elliot 1992 *Active Control of Sound*. London: Academic Press.
2. S. J. Elliot and P. A. Nelson 1994 *Noise/News International* **2**, 75–98. Active noise control.
3. D. R. Morgan 1980 *IEEE Transactions on Acoustics*, *Speech*, *and Signal Processing* **ASSP-28,** 454–467. An analysis of multiple correlation cancellation loops with a filter in the auxiliary path.
4. J. C. Burgess 1981 *Journal of Acoustical Society of America* **70**, 715–726. Active adaptive sound control in a duct: a computer simulation.
5. J. C. Doyle, B. A. Francis 1992 *Feedback Control Theory*. New York: Maxwell-Macmillan International.
6. B. A. Francis 1987 *Lecture Notes in Control and Information Science*. *A Course in H_∞ Control* **88** New York: Springer-Verlag.
7. D. K. Miu 1991 *Journal of Dynamic Systems*, *Measurements*, *and Control* **113**, 419–424. Physical interpretation of transfer function zeros for simple control systems with mechanical flexibilities.
8. K. J. Astrom, P. Hagander, J. Sternby 1984 *Automatica* **20**, 31–38. Zeros of sampled systems.
9. M. Morari and E. Zafiriou 1989 *Robust Process Control*. Englewood Cliffs, N.J.: Prentice-Hall.
10. G. F. Franklin, J. D. Powell, and A. Emani-Naeini 1994 *Feedback Control of Dynamic Systems*. Reading, Ma: Addison-Wesley.
11. J. G. Proakis and D. G. Manolakis 1992 *Digital Signal Processing*. New York: Maxwell-Macmillan International.
12. L. Ljung 1987 *System Identification*: *Theory for the User*. Englwood Cliffs, N.J.: Prentice-Hall.
13. B. Widrow and S. D. Stearns 1985 *Adaptive Signal Processing*. Englewood Cliffs, N.J.: Prentice-Hall.